Enhanced Information Recovery in 2D On- and Off-Resonance Nutation NQR using the Maximum Entropy Method *

Mariusz Maćkowiak and Piotr Kątowski

Institute of Molecular Physics, Polish Academy of Sciences, Smoluchowskiego 17, 60-179 Poznań, Poland

Z. Naturforsch. **51a**, 337–347 (1996); received January 22, 1996

Two-dimensional zero-field nutation NQR spectroscopy has been used to determine the full quadrupolar tensor of spin $-3/2$ nuclei in serveral molecular crystals containing the ^{35}Cl and ^{75}As nuclei. The problems of reconstructing 2D-nutation NQR spectra using conventional methods and the advantages of using implementation of the maximum entropy method (MEM) are analyzed. It is shown that the replacement of conventional Fourier transform by an alternative data processing by MEM in 2D NQR spectroscopy leads to sensitivity improvement, reduction of instrumental artefacts and truncation errors, shortened data acquisition times and suppression of noise, while at the same time increasing the resolution. The effects of off-resonance irradiation in nutation experiments are demonstrated both experimentally and theoretically. It is shown that off-resonance nutation spectroscopy is a useful extension of the conventional on-resonance experiments, thus facilitating the determination of asymmetry parameters in multiple spectrum. The theoretical description of the off-resonance effects in 2D nutation NQR spectroscopy is given, and general exact formulas for the asymmetry parameter are obtained. In off-resonance conditions, the resolution of the nutation NQR spectrum decreases with the spectrometer offset. However, an enhanced resolution can be achieved by using the maximum entropy method in 2D-data reconstruction.

Key words: Nuclear quadrupole resonance, 2D nutation spectroscopy, maximum entropy method, electric field gradient tensor.

1. Introduction

It is well known that pure nuclear quadrupole resonance (NQR) spectra of spin $-3/2$ nuclei do not allow determination of the asymmetry parameter η of the electric field gradient (EFG) tensor in a molecule due to degeneracy of the nuclear spin levels. For spin $I = 3/2$ it is not possible to determine the second-rank quadrupolar tensor from a conventional one-dimensional zero-field NQR, since the transition frequency depends on both the quadrupolar coupling constant e^2qQ/h and the asymmetry parameter η. Techniques that are used to determine η generally involve applying an external magnetic (Zeeman) field to remove the degeneracy of nuclear quadrupole states and produce orientation-dependent spectra. Recently Harbison et al. [1, 2] introduced a new method of two-dimensional zero-field nutation NQR spectroscopy for obtaining η in single crystal or powder samples. The advantage of this method is that no extra hardware (Helmholtz coils, etc.) is required but only some data processing in a computer. In the nutation NQR experiment, a two-dimensional time-domain signal $G(t, t_w)$ is detected during the free induction decay (FID) time t for varying radiofrequency (RF) pulse widths t_w. The first time period, characterized by a time variable t_w, is the duration of the radiofrequency excitation pulse. The second period is characterized by a time variable t and is the period of free precession of the quadrupolar nucleus at zero field. The direction of the RF field introduces an external quantization axis as the effective RF field, seen by a given nucleus, which depends on the relative orientation of the EFG tensor eigenframe with respect to the direction of the RF coil. Double Fourier transformation of the time-domain signal gives a two-dimensional spectrum $S(\omega_2, \omega_1)$, where the ω_2 dimension corresponds to a pure NQR spectrum, and the ω_1 dimension to a powder nutation spectrum consisting of three singularities at frequencies ν_1, ν_2 and ν_3. Asymmetry parameter can be obtained from ν_2 and ν_3 alone [1],

$$\eta - \frac{3(\nu_3 - \nu_2)}{\nu_3 + \nu_2}. \qquad (1)$$

* Presented at the XIIIth International Symposium on Nuclear Quadrupole Interactions, Providence, Rhode Island, USA, July 23–28, 1995.

Reprint requests to Prof. Dr. M. Maćkowiak.

0932-0784 / 96 / 0500-0337 $ 06.00 © – Verlag der Zeitschrift für Naturforschung, D-72072 Tübingen

Dieses Werk wurde im Jahr 2013 vom Verlag Zeitschrift für Naturforschung in Zusammenarbeit mit der Max-Planck-Gesellschaft zur Förderung der Wissenschaften e.V. digitalisiert und unter folgender Lizenz veröffentlicht: Creative Commons Namensnennung-Keine Bearbeitung 3.0 Deutschland Lizenz.

This work has been digitalized and published in 2013 by Verlag Zeitschrift für Naturforschung in cooperation with the Max Planck Society for the Advancement of Science under a Creative Commons Attribution-NoDerivs 3.0 Germany License.

Zum 01.01.2015 ist eine Anpassung der Lizenzbedingungen (Entfall der Creative Commons Lizenzbedingung „Keine Bearbeitung") beabsichtigt, um eine Nachnutzung auch im Rahmen zukünftiger wissenschaftlicher Nutzungsformen zu ermöglichen.

On 01.01.2015 it is planned to change the License Conditions (the removal of the Creative Commons License condition "no derivative works"). This is to allow reuse in the area of future scientific usage.

In derivation of (1) Harbison et al. neglected the offset of the spectrometer frequency from resonance. But very often the observed NQR spectra consist of some closely spaced lines (e.g. due to chemical inequivalence of quadrupolar nuclei); therefore one cannot fulfill the on-resonance condition for all the lines at a time and determine η for each line in single experiment. In the present work we show that a general expression for η, which includes frequency offset, can be easily obtained from the existing theory of NQR. We show how the 2D nutation NQR lineshape is modified in cases when the off-resonance effects are pronounced. Moreover, as the resonance offset is an easily controlled parameter, several NQR lines of the multiple spectrum may be excited simultaneously, thus facilitating the determination of asymmetry parameters for nuclei in inequivalent positions during the one single experiment. The off-resonance phenomena in 2D-NQR are very important from the practical point of view (determination of asymmetry parameters) and provide interesting information on dynamic properties of a quadrupolar spin system.

In real 2D-NQR experiments a noisy and strongly truncated set of pseudo-FID data is usually obtained. The direct application of Fourier transforms to 2D-NQR data has some serious limitations of fundamental nature, thus giving rise to difficulties in accurate spectral analysis and precise determination of singularities in a continuum-like powder pattern. With a view to developing efficient methodologies for η evaluation from polycrystalline specimens, we have applied an alternative approach that involves two-dimensional data processing and reconstruction of the 2D-nutation spectra by the maximum entropy method (MEM). We have shown that the replacement of conventional Fourier transforms by MEM leads to considerable improvements of the 2D-data reconstruction. Presented MEM spectra of short data sets, free of truncation effects and spurious lines, have much higher resolution and signal to noise ratio than traditional Fourier spectra. In this paper the theoretical results are confirmed experimentally 2D-nutation NQR spectra of several molecular compounds containing the ^{35}Cl and ^{75}As nuclei.

2. Transient Response of a Quadrupolar Spin System in Zero Applied Field to an RF Pulse

The expression for the NQR signal following a single RF pulse of length t_w was given by Pratt et al. [3] in the form

$$G(t, t_w) = A(t_w)\sin[\omega_0(t - t_w) + \beta(t_w)], \tag{2}$$

where

$$A(t_w) = [\omega_R/(4\xi^2)]\,R^2(\theta, \varphi)\sin\xi t_w \cdot (4\xi^2\cos^2\xi t_w + \Delta\omega^2\sin^2\xi t_w)^{1/2}. \tag{3}$$

The phase factor $\beta(t_w)$ depends on the evolution time t_w and the frequency offset $\Delta\omega$ as

$$\beta(t_w) = \arccos[u/\sqrt{u^2 + v^2}] \tag{4a}$$

with

$$u = \cos\xi t_w\cos\Delta\omega t_w + (\Delta\omega/2\xi)\sin\xi t_w\sin\Delta\omega t_w, \tag{4b}$$

$$v = -\cos\xi t_w\sin\Delta\omega t_w + (\Delta\omega/2\xi)\sin\xi t_w\cos\Delta\omega t_w. \tag{4c}$$

Here ξ, m and $R(\theta, \phi)$ are defined as

$$\xi = \tfrac{1}{2}\sqrt{4m^2 + \Delta\omega^2},$$
$$m = \omega_R R(\theta, \varphi)/4\sqrt{3 + \eta^2},$$
$$R(\theta, \varphi) = [4\eta^2\cos^2\theta + \sin^2\theta(9 + \eta^2 + 6\eta\cos 2\varphi)]^{1/2}. \tag{5}$$

Here $\Delta\omega = \omega - \omega_0$ is a distance of RF pulse frequency ω from NQR frequency ω_0, $\omega_R = 2\pi\gamma H_1$, θ and ϕ are polar angles related to the principal axes of the EFG tensor, and H_1 is the strength of the RF magnetic field. For ^{35}Cl nuclei the magnetogyric ratio is $\gamma = 417.2$ Hz/Gs.

The two-dimensional nutation NQR spectrum is obtained from double Fourier transform of (2):

$$S(\omega_2, \omega_1, \theta, \varphi) = \int_{-\infty}^{+\infty}\int_{-\infty}^{+\infty} G(t, t_w)\exp(i\omega_2 t)\exp(i\omega_1 t_w)\,dt\,dt_w. \tag{6}$$

In a polycrystalline powder all orientations of individual crystallites occur with equal probability, and the nutation spectrum can be calculated as a weighted average of (6) over all values of θ and ϕ:

$$S(\omega_2, \omega_1) = \int_0^{2\pi}\int_0^{\pi} |\sin\theta|\,S(\omega_2, \omega_1, \theta, \varphi)\,d\theta\,d\varphi. \tag{7}$$

Before considering our experimental results in detail, at this step we must notify, that (2) should be rewritten in the form

$$G(t, t_w) = A(t_w)\sin[\omega_0 t + \beta(t_w)] \tag{8}$$

in order to describe our off-resonance nutation experiment properly. The reason of that is a specific error

made in theoretical calculations published in the paper of Pratt et al. [3]: the expectation values of the operator $\langle I_q \rangle$ were defined in the laboratory frame of reference, but expansion coefficients $c_i(t_w)$ were calculated from the Schroedinger equation for the time interval $0 < t < t_w$, where a time-dependent Hamiltonian was defined in a frame rotating at the nuclear quadrupole frequency ω_0. Therefore, the calculated coefficients $c_i(t_w)$ should be multiplied by the factor $\exp(i\omega_i t_w)$ to transform them to the laboratory frame. Then the (11) in Pratt's paper [3] takes the form

$$\begin{aligned}\langle I_q \rangle &= \sum_{i,j} \overline{[c_i(t_w)\exp(-i\omega_i t_w)]}^{*} [c_j(t_w)\exp(i\omega_j t_w)] \\ &\quad \times \langle i | I_q | j \rangle \exp[-i(\omega_i - \omega_j)(t - t_w)] \qquad (9) \\ &= \sum_{i,j} \overline{[c_i(t_w)]}^{*} [c_j(t_w)] \langle i | I_q | j \rangle \exp[-i(\omega_i - \omega_j)t],\end{aligned}$$

which leads to our equation (8), as required by experimental results. The integral (6) appears to be soluble in closed from if (8) is converted to

$$G(t, t_w) = [\omega_R R^2(\theta, \varphi)/2\xi](u \sin \omega_0 t + v \cos \omega_0 t). \quad (10)$$

In nutation spectroscopy we are interested in how $G(t, t_w)$ varies with t_w and $\Delta\omega$. Before considering this in details, let us examine expression (10) for the signal height in two separate cases: 1) a pulse applied at exact resonance ($\Delta\omega = 0$), 2) off-resonance nutation spectroscopy ($\Delta\omega \neq 0$).

3. Two-dimensional Zero-field On-resonance Nutation NQR Lineshape

As follows from (10), for the case $\Delta\omega = 0$ the on-resonance nutation frequency ν_N^{on} is given by

$$\nu_N^{on} = \frac{1}{2\pi} \frac{\gamma H_1 R(\theta, \varphi)}{2\sqrt{3 + \eta^2}}. \qquad (11)$$

Two characteristic nutation frequencies corresponding to different crystallite orientations may be distinguished and applied to determine η from (1):

For $\theta = 90°$, $\phi = 90°$:

$$\nu_2^{on} = \frac{1}{2\pi} \frac{\gamma H_1 (3 - \eta)}{2\sqrt{3 + \eta^2}}. \qquad (12a)$$

For $\theta = 90°$, $\phi = 0°$:

$$\nu_3^{on} = \frac{1}{2\pi} \frac{\gamma H_1 (3 + \eta)}{2\sqrt{3 + \eta^2}}. \qquad (12b)$$

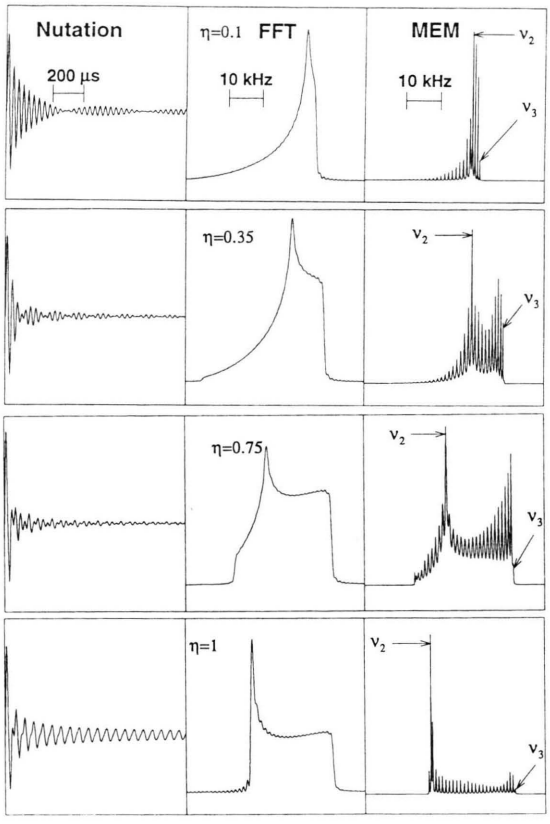

Fig. 1. Computer-simulated on-resonance nutation interferograms, their Fourier-transforms (FFT) and corresponding MEM spectrum (in the ω_1 dimension) for a spin-3/2 nucleus as a function of the asymmetry parameter. The Fourier lineshapes were obtained by numerical integration of (13) using 200 values of θ over an interval of $0-\pi$ rad and 400 values of ϕ over 0 to 2π rad, $H_1 = 120$ Gs, 1024 data points were taken before Fourier transformation.

In a polycrystalline powder the two-dimensional nutation lineshape is obtained by integration over θ and ϕ, followed by double-Fourier transformation:

$$\begin{aligned}&S(\omega_1, \omega_2) \\ &= \int_0^{2\pi} \int_0^{\pi} \int_{-\infty}^{+\infty} \int_{-\infty}^{+\infty} R(\theta, \varphi) \sin\theta \sin\left[\frac{\gamma H_1}{2} \frac{R(\theta, \varphi)}{\sqrt{3 + \eta^2}} t_w\right] \\ &\quad \cdot \sin(\omega_0 t) \exp(i\omega_1 t_w) \exp(i\omega_2 t)\, dt\, dt_w\, d\theta\, d\varphi. \qquad (13)\end{aligned}$$

This expression leads to a powder pattern in the ω_1 dimension. We have calculated the lineshape of this powder pattern as a function of the asymmetry parameter (Figure 1). The powder patterns calculated by the Fourier transform reveal the singularities ν_2 and ν_3 predicted by the analytical theory of Harbison et al.

[1]. However, as demonstrated in Fig. 1, the Fourier method does not lead to a clear resolution even in the numerical simulation. This may lead to severe inconveniences in the interpretation of the spectra. The problem we are addressing in this paper is to find suitable procedures to process two-dimensional data. In the next section we show that the data processing by the maximum entropy method (MEM) leads to considerable improvements of 2D-data reconstruction.

4. Reconstruction of Two-dimensional NQR Nutation Spectrum by Maximum Entropy Method

The Maximum Entropy Method (MEM) is a mathematical technique based on rigorous probability theory that gives the best estimate of the underlying distribution in a spectrum from limited data. MEM can only recover information which is present to some degree in the original data. One of the strengths of the method is that it will reproduce only the minimum of structure needed to fit the data adequately, so that MEM results are largely free of artefacts. A MEM result consists of the most probable spectrum, which will be the spectrum of greatest entropy best fitting the data, within the experimental noise. The idea of the MEM procedure for 2D-nutation NQR purposes is to find a set of nutation lineshapes which are consistent with the experimental pseudo-FID. The criterion for the selection of a lineshape out if this set is the minimum of the information content, or equivalently the maximum of the entropy. More details of the method have been reported in [4–8].

The nutation spectrum reconstructed by fitting the experimental pseudo-FID is considered as a set of positive numbers $\{P_j\}, j = 1, 2, \ldots, K$, which are to be determined. According to the information theory, the Shannon entropy H is a measure of the amount of uncertainty in the distribution of propabilities $P_1, \ldots, P_K$.

$$H = -\sum_{j=1}^{K} P_j \log(P_j) . \tag{14}$$

The distribution of P_j that most honestly describes reality is the one that maximizes the entropy H. The discrete pseudo-FID data set, $\{G_w\}$, representing the individual interferograms can be expressed as

$$G_w = \sum_{j=1}^{K} G_{w,j} P_j \pm \sigma_w ; \quad w = 1, 2, \ldots, M , \tag{15}$$

where σ_w is the standard deviation of the noise, and M and K are the numbers of points in the pseudo-FID and in the resulting nutation spectrum, respectively. The individual interferograms, as follows from (7), are given by

$$G_{w,j} = \int_0^{\pi} \mathrm{d}\theta \int_0^{2\pi} \mathrm{d}\varphi \sin\theta \, R(\theta, \varphi) \sin[\omega_{N,j} t_w] . \tag{16}$$

The actual data set G_w is to be compared with the simulated data according to

$$\Gamma_w = \sum_{j=1}^{K} G_{w,j} P_j . \tag{17}$$

The misfit between the actual data set $\{G_w\}$ and the simulated set $\{\Gamma_w\}$ is characterized by the least-squares criterion of statistics

$$\chi^2 = \sum_{w=1}^{M} \frac{(\Gamma_w - G_w)^2}{\sigma_w^2} . \tag{18}$$

In this paper we use the Burg algorithm [7] to select the feasible lineshape that maximizes the entropy. The powder spectrum obtained by this method can be written in the form

$$G(v) = P_m \left| 1 - \sum_{k=1}^{m} a_k \exp(2\pi i k v) \right|^{-2} . \tag{19}$$

The coefficients a_k are so-called filter coefficients of a linear prediction filter of size m, and P_m is the prediction error of the filter. A MEM spectrum is reconstructed by repeatedly taking revised trial spectra which fit the data better and better to converge on the most probable spectrum.

As seen in Fig. 1, the MEM for the analysis of a complex NQR spectrum is superior to the usual FFT method. One of the most important aspects of the MEM application in 2D spectroscopy is the elimination of the so-called t_1 noise in the ω_1 spectrum domain, a phenomenon resulting from truncation (incomplete data) in the t_1 time domain. A relevant point for profitable use of the MEM is the estimate of the size of a linear prediction filter m that gives the best spectrum with the highest possible resolution. The optimum condition depends on the noise characteristics, NQR spectral structure, and desired optimal final resolution without introducing spurious frequencies. A 2D nutation spectrum of powders consists of closely spaced continuum-like frequencies with short data sets. Therefore a large value of m is needed ot obtain the best resolution. In our case remarkably narrow peaks with good stability, independent of the size m,

and with good overall reproduction of the envelope of the nutation spectrum were obtained from $m \cong 0.95\,N$, where N is the number of the data points in the time domain.

5. Off-resonance Effects in 2D Nutation Spectroscopy

Let us now consider the response of the quadrupolar spin $I = 3/2$ system in zero-applied field to the RF off-resonance irradiation with the frequency offset $\Delta\omega$. An important consequence of off-resonance irradiation is that the modulation of the observed FID changes from amplitude modulation into phase modulation. Moreover, the outcome of the off-resonance nutation experiments depends on the data acquisition procedure.

Now, let us examine the two cases of NQR data acquisition possible in a pulsed NQR spectrometer. In the first case the aquisition of a free induction decay (FID) signal starts immediately after the RF pulse is turned off (we neglect the spectrometer dead time for simplicity) and in (10) we have $t = t_w$. Then, after some algebra, we find

$$G(t_w) = [\omega_R R^2(\theta, \varphi)/4\xi]\,\Delta\omega\,(1 - \cos 2\xi t_w)\,. \quad (20)$$

The integral (6) of (20) is trivial, and we obtain single nutation spectrum at the frequency given by

$$\nu_N^{\text{off}} = \xi/\pi = \sqrt{(\nu_N^{\text{on}})^2 + (\Delta\nu)^2}\,, \quad (21)$$

where ν_N^{on} is the on-resonance nutation frequency given by (11) and $\Delta\nu$ is the resonance offset. As in the case of on-resonance nutation, the asymmetry parameter has a large effect on the evolution of the spin system during the off-resonance RF excitation. After calculation of the two characteristic nutation frequencies corresponding to different crystalline orientations we obtain the following evaluation formula for the asymmetry parameter:

$$\eta = \frac{3\left[\sqrt{(\nu_3^{\text{off}})^2 - (\Delta\nu)^2} - \sqrt{(\nu_2^{\text{off}})^2 - (\Delta\nu)^2}\right]}{\sqrt{(\nu_3^{\text{off}})^2 - (\Delta\nu)^2} + \sqrt{(\nu_2^{\text{off}})^2 - (\Delta\nu)^2}}\,. \quad (22)$$

Note that when $\Delta\nu = 0$ we obtain the equation (1) previously published by Harbison et al. [1]. In a powder sample the characteristic frequencies ν_2 and ν_3 appear as powder pattern singularities.

Now let us proceed to the second possible mode of nutation experiment, when the acquisition of FID signal starts at some constant delay t_0 after the RF pulse has been turned on ($t_0 > t_w$). On substitution $t = t_0$ the (10) can now be converted to

$$\begin{aligned} G(t_w) = \frac{R^2(\theta, \varphi)\,\omega_R}{8\xi} \Bigg\{ \Bigg[\Bigg(1 + \frac{\Delta\omega}{2\xi}\Bigg) \sin(2\xi - \Delta\omega)\,t_w \\ + \Bigg(1 - \frac{\Delta\omega}{2\xi}\Bigg) \sin(2\xi + \Delta\omega)\,t_w \\ + \frac{\Delta\omega}{\xi} \sin(\Delta\omega\,t_w) \Bigg] \sin\omega_0 t_0 \\ + \Bigg[\Bigg(1 - \frac{\Delta\omega}{2\xi}\Bigg) \cos(2\xi + \Delta\omega)\,t_w \\ - \Bigg(1 + \frac{\Delta\omega}{2\xi}\Bigg) \cos(2\xi - \Delta\omega)\,t_w \\ + \frac{\Delta\omega}{\xi} \cos(\Delta\omega\,t_w) \Bigg] \cos\omega_0 t_0 \Bigg\}. \end{aligned} \quad (23)$$

Here again the Fourier transform of (23) is straightforward and gives a nutation spectrum consisting of three lines (as predicted by Sinjavsky [9, 10]). The line at the frequency offset $\Delta\nu$ is independent of the EFG parameters and does not provide any information on the EFG symmetry. The frequencies of two other lines are given by

$$\nu_N^{\text{off}} = \sqrt{(\nu_N^{\text{on}})^2 + (\Delta\nu)^2} \pm \Delta\nu\,. \quad (24)$$

Thus the evaluation formula for the asymmetry parameter is of the form

$$\eta = \frac{3\left[\sqrt{(\nu_3^{\text{off}})^2 \pm 2\nu_3^{\text{off}}\Delta\nu} - \sqrt{(\nu_2^{\text{off}})^2 \pm 2\nu_2^{\text{off}}\Delta\nu}\right]}{\sqrt{(\nu_3^{\text{off}})^2 \pm 2\nu_3^{\text{off}}\Delta\nu} + \sqrt{(\nu_2^{\text{off}})^2 \pm 2\nu_2^{\text{off}}\Delta\nu}}\,. \quad (25)$$

For a on-resonance nutation experiment ($\Delta\nu = 0$), (25) also reduces to (1). Let us define the relative decrease of spectral resolution of the off-resonance nutation NQR spectrum by

$$r[\%] = 100\left(1 - \frac{\nu_3^{\text{off}} - \nu_2^{\text{off}}}{\nu_3^{\text{on}} - \nu_2^{\text{on}}}\right), \quad (26)$$

where $\nu_{2,3}^{\text{on}} = (1/2\pi)\,\omega_R(3 \pm \eta)/(2\sqrt{3 + \eta^2})$ and $\nu_{2,3}^{\text{off}} = \sqrt{(\nu_{2,3}^{\text{on}})^2 + (\Delta\nu)^2}$ refer to characteristic nutation frequencies observed in on-resonance and off-resonance experiments, respectively. Figure 2 shows the theoretical variation of decrease of the nutation spectrum resolution with frequency offset $\Delta\nu$, calculated using (26) with $H_1 = 70$ Gs (the latter value was estimated from experimentally determined 90° pulse length of 8 μs). As we see, the decrease in nutation spectrum resolution is almost independent of η. For moderate frequency offset, $\Delta\nu = 10$ kHz, the resolution is decreased by less than 10%. However, for frequency

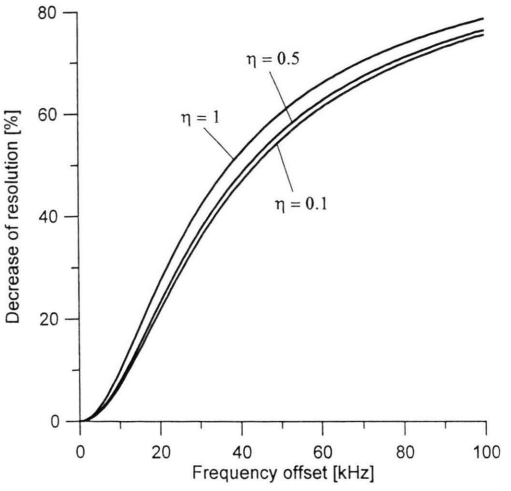

Fig. 2. Theoretical variation of the decrease of a nutation NQR spectral resolution as a function of spectrometer frequency offset from resonance.

offset as high as 100 kHz the nutation spectrum resolution will be decreased by rather unacceptable value of 80%.

6. Experimental

Two-dimensional nutation experiments were carried out using the home-built pulsed spectrometer equipped with automatically tuned probe-head system operating in the frequency range 0.5–150 MHz [11]. The probe-head has been inserted into the Oxford CF 1200 helium-flow cryostat. The dedicated command-driven operating system software is designed to meet specific NQR requirements and incorporates the 2D-FFT/MEM data-processing system. Special attention has to be given to three experimental factors of critical importance: a) temperature stability, b) RF field homogeneity, c) power level stability. As in other forms of nutation spectroscopy, the RF homogeneity over the sample volume is of critical importance. The sample of small volume are placed inside a long double-wired sample coil to increase RF homogeneity without increasing coil inductance. The RF coil is typically 40 mm long and 10 mm inner diameter. The sample was packed in a 7 mm i.d. glass tube 15 mm long and was placed in the center of the RF coil. The stability of RF power has to be controlled. It is usually necessary to reduce the transmitter power to 600 W to prevent probe arcing towards the end of the nutation experiment, when pulse length is close to 400 μs. We have noticed that for such a long pulse the nonlinearity as small as 3% leads to significant distortions of the spectra and smearing out the singularities. The major consideration is sample heating because the thermal fluctuations of greater than 0.2 K severely distort the spectra. Recycle delays between transients were much longer than is necessary to allow the spins to relax and the probe was actively gas-cooled. Moreover, we have modified the simple one-pulse sequence by introducing the second pulse of duration $t_{w\,\max} - t_w$ [8]. Thus the experiment was carried out at constant RF power dissipating in the resonance circuit.

7. Results and Discussion

The experimental ^{35}Cl 2D on-resonance nutation spectrum obtained as 2D-FT $S(F_1, F_2)$ of the recorded data set $G(t, t_w)$ for the line $\nu_{NQR} = 36.772$ MHz at 77 K in polycrystalline 1,3,5-trichloro-2,4,6-triazine ($C_3N_3Cl_3$) is shown in Figure 3. The contour map in the F_1 *vs.* F_2 plane is also shown. In the second time-dimension (t) 1024 data points were acquired with 1.6 μs sampling period; before FT those data were routinely zero-filled up to 4096 points. In the first time-dimension (t_w) 162 data points were acquired with the exciting pulse incremented by 2 μs and zero-filling up to 2048 points. FID was accumulated 50 times for each step in the t_w dimension. A nutation spectrum has been obtained at an RF pulse of $H_1 = 120$ Gs. Characteristic singularities ν_2 and ν_3 are seen in the spectrum but their exact positions have to be determined by the maximum entropy method. As shown in Fig. 4, the MEM analysis of a complex NQR spectrum is superior to the usual FFT method. The t_1-noise in the F_1 spectrum is reduced and the high resolution allowing the exact determination of singularities is obtained. From the positions of the ν_2 peak (the highest-intensity peak of the MEM spectrum) and the ν_3 peak (the high-frequency peak) we determined the asymmetry parameter to be 0.222 ± 0.005 [12]. This result can be interpreted in terms of the effect of the ring nitrogen on the double-bond character of the carbon-chloride bond. In $C_3N_3Cl_3$ this effect should be quite pronounced, as there are three such nitrogens in the ring. The asymmetry is roughly proportional to the double bond character of the halogen bond, thus the value of η is so high.

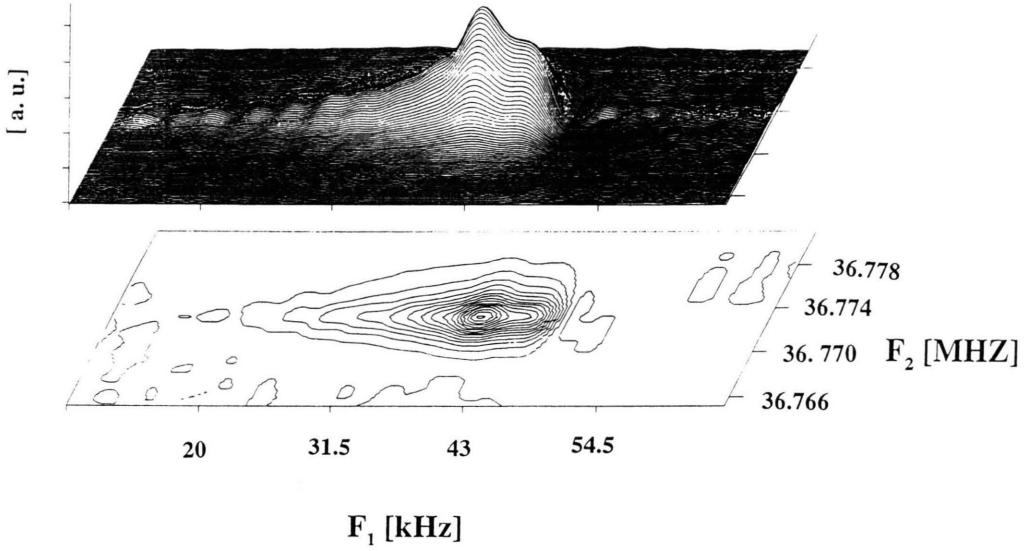

Fig. 3. 2D zero-field on-resonance nutation spectrum of ^{35}Cl in 1,3,5-trichloro-2,4,6-triazine ($C_3N_3Cl_3$) obtained at 77 K for ν_{NQR} = 36.772 MHz. Contour map of the 2D-nutation spectrum in the F_1 *vs.* F_2 plane is also shown.

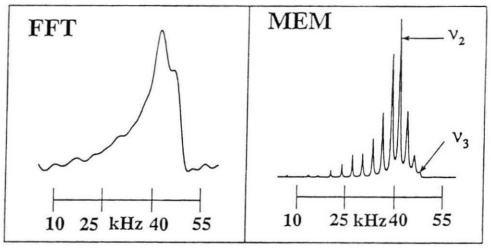

Fig. 4. Fourier transform of the on-resonance nutation spectrum and corresponding MEM spectrum (the slices through the 2D spectrum parallel to the F_1 axis at $F_2 = \nu_{NQR}$) obtained at 77 K for ν_{NQR} = 36.772 MHz in $C_3N_3Cl_3$. The linear prediction filter used to obtain the MEM spectrum from N = 162 time-domain data points was m = 0.95 N.

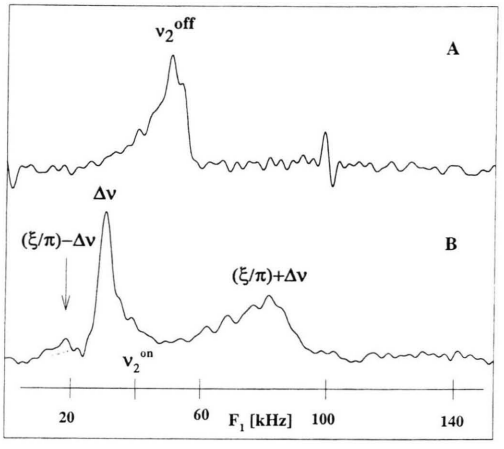

Fig. 5. Effects of different acquisition procedures on the off-resonance nutation spectra in $C_3N_3Cl_3$. The frequency offset is $\Delta\nu$ = 32 kHz. A) one-line nutation spectrum with shifted frequency as predicted by (21) (FT absorption spectrum), B) three-line spectrum with frequency predicted by (24) (FT power spectrum is shown to avoid phasing problems).

The ^{35}Cl NQR spectrum of $C_3N_3Cl_3$ exhibits two lines with an intensity ratio of 1:2 and frequencies $\nu^{(1)}_{NQR}$ = 36.772 MHz and $\nu^{(2)}_{NQR}$ = 36.740 MHz at 77 K. By setting the spectrometer frequency at 36.772 MHz the frequency offset of 32 kHz for the second line is obtained. As predicted by (21), the off-resonance line has a higher overall nutation frequency (Figure 5). In the F_1 dimension characteristic harmonic frequencies of the off-resonance nutation frequency are observed also (Figure 5(a)). The Fourier-transform of a highly non-linear term of 2ξ in (20) is responsible for this effect. The off-resonance nutation spectrum, shown in Fig. 5(a), reveals less pronounced structure, what we might expect from the plot in Fig. 2 which shows, that for the frequency offset of 32 kHz the nutation spectrum decreases by about 35%. Using experimental values of ν_2^{off} and ν_3^{off} determined by the MEM we evaluated the value of asymmetry parameter in $C_3N_3Cl_3$ from the off-resonance spectrum using (22).

The obtained value of 0.222 is identical with that obtained in on-resonance nutation experiment. Even though the resolution of the off-resonance spectrum decreases with the spectrometer offset, an enhanced resolution can be achieved by using the MEM and an appropriate formula for determination of η. Figure 5(b) shows the outcome of off-resonance nutation experiment using different acquisition procedure. As predicted by the theory, three lines are observed when the data acquisition is triggered by the beginning of the RF pulse. In both cases, however, using an appropriate formula ((22) or (25)) it is possible to determine the asymmetry parameter of the EFG tensor.

Figure 6 shows off-resonance (a) and on-resonance (b) nutation ^{35}Cl NQR spectra of $TiCl_4$ for FID data acquisition starting at RF pulse turn-off (mode 1). At 77 K the ^{35}Cl NQR spectrum of $TiCl_4$ consists of four lines. Two of them were measured in our experiment. Spectrometer frequency was set exactly on the upper line of frequency 6.0805 MHz. The lower line occurs at 6.0376 MHz, therefore both on-resonance and 43 kHz off-resonance nutation NQR spectra could be obtained in a single experiment. The on-resonance nutation spectrum at 24.7 kHz has a typical powder pattern with a pronounced shoulder on its right side, indicating a significant asymmetry parameter. The exact positions of ν_2 and ν_3 singularities were determined by processing of the nutation interferogram with a MEM algorithm and the value of the asymmetry parameter was calculated from (1) to be 0.18. We shall discuss this value in terms of molecular structure elsewhere. The off-resonance nutation spectrum, shown in Fig. 6(a), is shifted towards higher frequencies ($\nu_2^{\text{off}} = 49.7$ kHz) according to (21). Moreover, this off-resonance spectrum does not reveal a pronounced shoulder, what we might expect from the plot in Fig. 2 which shows, that for the frequency offset of 43 kHz the resolution of nutation spectrum decreases by about 50%. In Fig. 7(b) the off-resonance nutation spectrum is shown for data acquisition starting at constant delay after RF pulse turn-on (mode 2). Here we can see three nutation lines occurring at frequencies: $\xi/\pi - \Delta\nu = 49.7\text{ kHz} - 43\text{ kHz} = 6.7$ kHz, $\Delta\nu = 43$ kHz and $\xi/\pi + \Delta\nu = 49.7\text{ kHz} + 43\text{ kHz} = 92.7$ kHz according to (24). Note, that the form of nutation NQR spectra obtained from on-resonance data is independent of the above mentioned data acquisition mode. Although the off-resonance data acquisition in mode 2 is less practical than in mode 1 because of more complicated, triplet nutation spectrum involved, we report this result in order to validate theoretical assumptions that we have made by

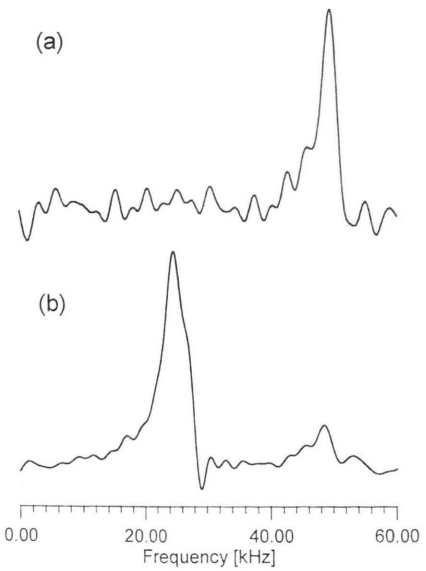

Fig. 6. Nutation ^{35}Cl NQR spectra of $TiCl_4$ obtained for the lower NQR line with spectrometer frequency set 43 kHz off-resonance (a), and for the upper NQR line with spectrometer frequency set on-resonance (b). Both nutation spectra were obtained using data acquisition mode 1 (see text).

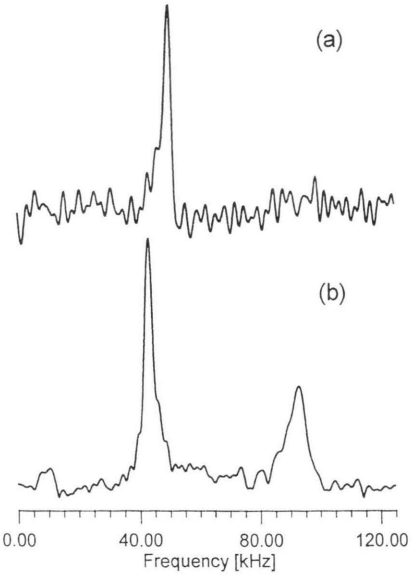

Fig. 7. Nutation ^{35}Cl NQR spectra of $TiCl_4$ obtained using data acquisition mode 1 – (a), and mode 2 – (b) (see text). Both nutation spectra were obtained for the lower NQR line with spectrometer frequency set 43 kHz off-resonance.

changing the form of (2). As a matter of fact, it was not necessary to perform the real experiment in mode 2, because this mode of data acquisition could be easily software-simulated when data collected in mode 1 were processed by 2D-FFT program. We have to stress out that the uncorrected Pratt's theory [3] leads to some controversies in the literature and is responsible for misinterpretation of the three-line nutation spectrum [9].

As shown in Fig. 8, the dependence of the off-resonance nutation frequency on the frequency offset $\Delta\nu$ follows (21). The NQR spectrum in $TiCl_4$ consists of four lines spread over 100 kHz. Thus the off-resonance effects can be observed in wider frequency range.

2D FT/MEM NQR on-resonance nutation spectroscopy in polycrystalline 2,6-dichlorophenol demonstrated the effect of intramolecular hydrogen bonding on the electric field gradient asymmetry parameter. At 284 K two ^{35}Cl NQR lines were observed at frequencies $\nu_{NQR}^{(1)} = 34.452$ MHz and $\nu_{NQR}^{(2)} = 34.743$ MHz. The lower frequency line is assigned to a hydrogen bonded orthochlorine, invoking intramolecular hydrogen bonding. 2D-nutation spectra were obtained for both of these resonances to study the effect of hydrogen bonding on the asymmetry parameter. The spectrometer frequency was set exactly on resonance in both cases. The lineshapes of the nutation spectra in the F_1 dimension are very complex and indicate considerable and different values of asymmetry parameter for the two chlorines (Figure 9). For the high-frequency line

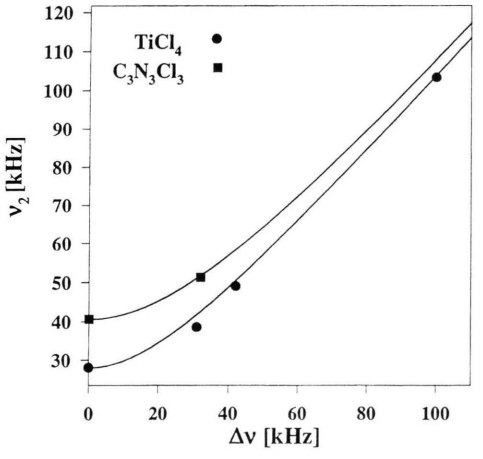

Fig. 8. Dependence of the off-resonance nutation frequency ν_2 on the frequency offset $\Delta\nu$ in $C_3N_3Cl_3$ and $TiCl_4$. The solid line is the theoretical dependence given by (21).

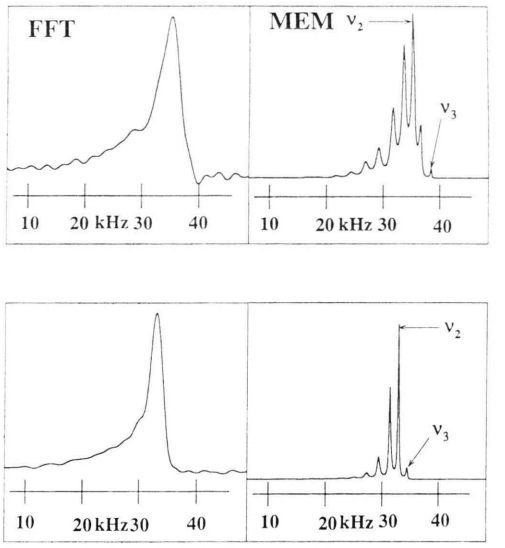

Fig. 9. 2D on-resonance Fourier transforms and corresponding MEM nutation spectra of 2,6-dichlorophenol at $T = 284$ K for $\nu_{NQR} = 34.743$ MHz (upper spectrum) and $\nu_{NQR} = 34.452$ MHz (lower spectrum). The effect of intramolecular hydrogen bonding on the asymmetry parameter is clearly demonstrated. The linear prediction filter used to obtain the MEM spectra from $N = 202$ data points was $m = 0.95\ N$.

the nutation spectrum in the F_1 dimension is broader and shows a characteristic shoulder at high-frequency end of the nutation spectrum indicating the larger asymmetry parameter. As seen in Fig. 9, the MEM for the analysis of complex NQR spectrum has proven to be remarkably adaptive and superior over the usual FT method. The chlorine atom that is *ortho* to the OH group and involved in hydrogen bonding (i.e. corresponding to the low-frequency line) gave an asymmetry parameter of $\eta = 0.065$ while the other chlorine (i.e. corresponding to the high-frequency line) gave a higher value of $\eta = 0.140$. Thus the formation of the hydrogen bond leads to a decrease of the NQR frequency and asymmetry parameter. The correlation between the proton transfer in hydrogen bonds and the values of η may therefore be studied by 2D-nutation FT/MEM spectroscopy and discussed in terms of hydrogen bonding and chemical bonds theory.

2D-nutation on-resonance spectroscopy has been applied for determination the EFG tensor at the ^{75}As site in antiferroelectric phase of polycrystalline ammonium dihydrogen arsenate (ADA). By determining the asymmetry parameter one can obtain information on the proton arrangement in this class of hydrogen

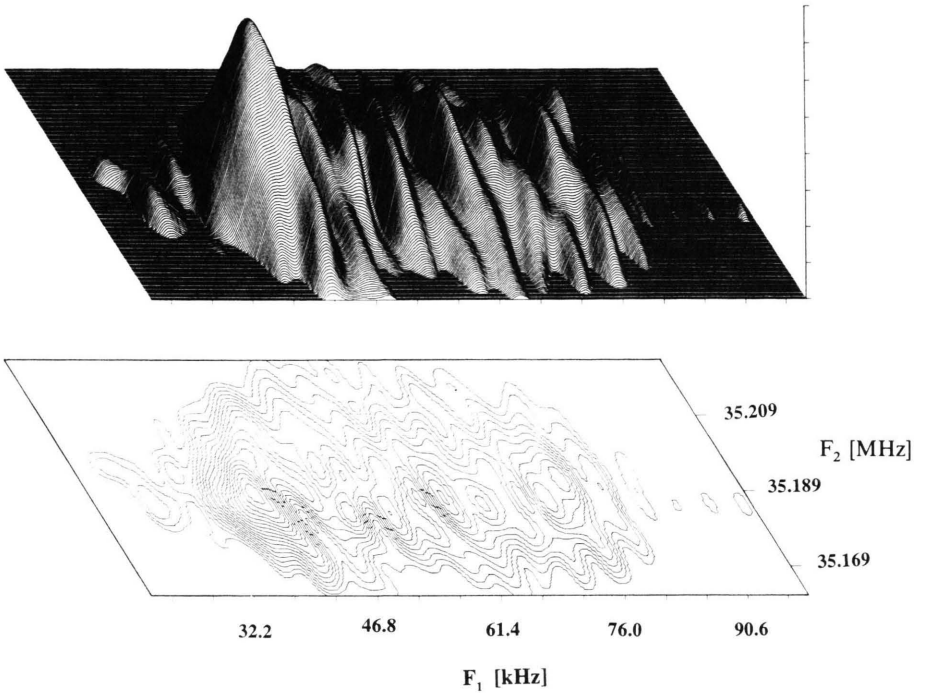

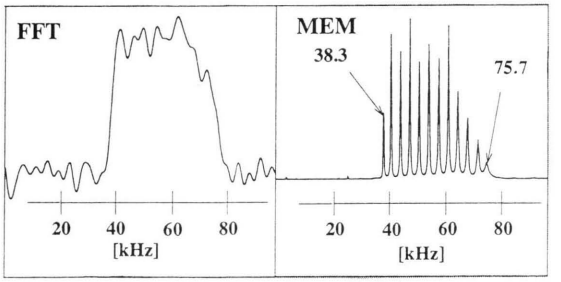

Fig. 10. a) Contour map of the 2D spin-echo on-resonance nutation spectrum of ^{75}As in polycrystalline ADA at 77 K. b) 2D spin-echo nutation FT spectrum and its corresponding MEM spectrum obtained at 77 K, $\nu_{NQR} = 35.180$ MHz. The linear prediction filter used to obtain the MEM spectrum from $N = 273$ data points was $m = 0.95\ N$.

bonded crystals. Due to the large NQR linewidth the conventional nutation spectroscopy is useless and an alternative approach by introducing a refocussing pulse [2] was used. The virtue of this refocussing pulse is that it allows acquisition of nutation spectra from samples with arbitrary inhomogeneous linewidth. A contour map of the FT-nutation spectrum in the F_1 *vs.* F_2 plane is shown in Figure 10(a). Characteristic singularities are seen as sharp edges in the low- and high-frequency end of the nutation spectrum. From the positions of the singularities in the MEM spin-echo nutation spectrum (Fig. 10(b)) we determined the asymmetry parameter $\eta = 1$. This result presents a direct proof that the antiferroelectric proton ordering is correct. The information on the local electron environment of the nucleus, obtained by 2D-NQR spin-echo nutation spectra reconstructed by the maximum entropy method, is valuable for the exploration of molecular structure and dynamics in the ADA-based proton glasses and hydrogen bonded ferroelectrics [13].

The result presented here clearly indicate that 2D on- and off-resonance zero-field nutation NQR spectroscopy with the MEM data-procedure permits us to achieve enhanced spectra resolution and provides a convenient approach for the evaluation of η. This fact favours the application of MEM as a new class of two-dimensional data processing method.

Acknowledgements

This research has been supported by the KBN grant no. PB 722/P3/93/04. The technical assistance of Dr. M. Ostafin is highly appreciated.

[1] G. S. Harbison, A. Slokenbergs, and T. M. Barbara, J. Chem. Phys. **90,** 5292 (1989).
[2] G. S. Harbison and A. Slokenbergs, Z. Naturforsch. **45a,** 575 (1990).
[3] J. C. Pratt, P. Raghunathan, and C. A. McDowell, J. Magn. Reson. **20,** 313 (1975).
[4] S. F. Gull and G. J. Daniell, Nature **272,** 686 (1978).
[5] E. D. Laue, J. Skilling, J. Staunton, S. Sibisi, and R. G. Brereton, J. Magn. Reson. **62,** 437 (1985).
[6] J. C. Hoch, J. Magn. Reson. **64,** 436 (1985).
[7] M. Maćkowiak and P. Kątowski, Appl. Magn. Reson. **5,** 433 (1993).
[8] H. Robert, D. Pusiol, E. Rommel, and R. Kimmich, Z. Naturforsch. **49a,** 35 (1994).
[9] N. Sinjavsky, Sol. State Phys. **33,** 3255 (1991).
[10] M. Ostafin, M. Maćkowiak, P. Kątowski, and N. Sinjavsky, Mol. Phys. Rep. (in press).
[11] M. Ostafin, M. Maćkowiak, and M. Bojarski, Z. Naturforsch. **49a,** 42 (1994).
[12] M. Maćkowiak, P. Kątowski, and M. Ostafin, J. Mol. Struct. **345,** 173 (1995).
[13] J. Dolinsek, F. Milia, G. Papavassiliou, G. Papantopoulos, and R. Rumm, J. Magn. Reson. **A114,** 147 (1995).